



# Hybrid Solid Oxide Fuel Cell/Gas Turbine System Design for High Altitude Long Endurance Aerospace Missions

*Ananda Himansu  
Taitech, Inc., Beavercreek, Ohio*

*Joshua E. Freeh, Christopher J. Steffen, Jr.,  
Robert T. Tornabene, and Xiao-Yen J. Wang  
Glenn Research Center, Cleveland, Ohio*

## NASA STI Program . . . in Profile

Since its founding, NASA has been dedicated to the advancement of aeronautics and space science. The NASA Scientific and Technical Information (STI) program plays a key part in helping NASA maintain this important role.

The NASA STI Program operates under the auspices of the Agency Chief Information Officer. It collects, organizes, provides for archiving, and disseminates NASA's STI. The NASA STI program provides access to the NASA Aeronautics and Space Database and its public interface, the NASA Technical Reports Server, thus providing one of the largest collections of aeronautical and space science STI in the world. Results are published in both non-NASA channels and by NASA in the NASA STI Report Series, which includes the following report types:

- **TECHNICAL PUBLICATION.** Reports of completed research or a major significant phase of research that present the results of NASA programs and include extensive data or theoretical analysis. Includes compilations of significant scientific and technical data and information deemed to be of continuing reference value. NASA counterpart of peer-reviewed formal professional papers but has less stringent limitations on manuscript length and extent of graphic presentations.
- **TECHNICAL MEMORANDUM.** Scientific and technical findings that are preliminary or of specialized interest, e.g., quick release reports, working papers, and bibliographies that contain minimal annotation. Does not contain extensive analysis.
- **CONTRACTOR REPORT.** Scientific and technical findings by NASA-sponsored contractors and grantees.

- **CONFERENCE PUBLICATION.** Collected papers from scientific and technical conferences, symposia, seminars, or other meetings sponsored or cosponsored by NASA.
- **SPECIAL PUBLICATION.** Scientific, technical, or historical information from NASA programs, projects, and missions, often concerned with subjects having substantial public interest.
- **TECHNICAL TRANSLATION.** English-language translations of foreign scientific and technical material pertinent to NASA's mission.

Specialized services also include creating custom thesauri, building customized databases, organizing and publishing research results.

For more information about the NASA STI program, see the following:

- Access the NASA STI program home page at <http://www.sti.nasa.gov>
- E-mail your question via the Internet to [help@sti.nasa.gov](mailto:help@sti.nasa.gov)
- Fax your question to the NASA STI Help Desk at 301-621-0134
- Telephone the NASA STI Help Desk at 301-621-0390
- Write to:  
NASA STI Help Desk  
NASA Center for AeroSpace Information  
7121 Standard Drive  
Hanover, MD 21076-1320



# Hybrid Solid Oxide Fuel Cell/Gas Turbine System Design for High Altitude Long Endurance Aerospace Missions

*Ananda Himansu  
Taitech, Inc., Beavercreek, Ohio*

*Joshua E. Freeh, Christopher J. Steffen, Jr.,  
Robert T. Tornabene, and Xiao-Yen J. Wang  
Glenn Research Center, Cleveland, Ohio*

Prepared for the  
Fourth International Conference on Fuel Cell Science, Engineering and Technology  
sponsored by the American Society of Mechanical Engineers  
Irvine, California, June 19-21, 2006

National Aeronautics and  
Space Administration

Glenn Research Center  
Cleveland, Ohio 44135

## Acknowledgments

The authors are sincerely grateful to James Walker and Jeffrey Berton, both of NASA Glenn Research Center, for their painstaking reviews of this paper and for their valuable suggestions. The authors also wish to thank the anonymous ASME reviewers for their suggested improvements. We are grateful to the authors of the Cantera software library, for providing quality open-source freeware. Ananda Himansu was supported in this work by funds from the Aircraft Fuel Cell Power System (AFCPS) program at Glenn Research Center, through Contract NAS3-03072.

This report contains preliminary findings,  
subject to revision as analysis proceeds.

This work was sponsored by the Fundamental Aeronautics Program  
at the NASA Glenn Research Center.

*Level of Review:* This material has been technically reviewed by technical management.

Available from

NASA Center for Aerospace Information  
7121 Standard Drive  
Hanover, MD 21076-1320

National Technical Information Service  
5285 Port Royal Road  
Springfield, VA 22161

Available electronically at <http://gltrs.grc.nasa.gov>

# Hybrid Solid Oxide Fuel Cell/Gas Turbine System Design for High Altitude Long Endurance Aerospace Missions

Ananda Himansu  
Taitech, Inc.  
Beavercreek, Ohio 45430

Joshua E. Freeh, Christopher J. Steffen, Jr., Robert T. Tornabene, and Xiao-Yen J. Wang  
National Aeronautics and Space Administration  
Glenn Research Center  
Cleveland, Ohio 44135

## ABSTRACT

A system level analysis, inclusive of mass, is carried out for a cryogenic hydrogen fueled hybrid solid oxide fuel cell and bottoming gas turbine (SOFC/GT) power system. The system is designed to provide primary or secondary electrical power for an unmanned aerial vehicle (UAV) over a high altitude, long endurance mission. The net power level and altitude are parametrically varied to examine their effect on total system mass. Some of the more important technology parameters, including turbomachinery efficiencies and the SOFC area specific resistance, are also studied for their effect on total system mass. Finally, two different solid oxide cell designs are compared to show the importance of the individual solid oxide cell design on the overall system. We show that for long mission durations of 10 days or more, the fuel mass savings resulting from the high efficiency of an SOFC/GT system more than offset the larger powerplant mass resulting from the low specific power of the SOFC/GT system. These missions therefore favor high efficiency, low power density systems, characteristics typical of fuel cell systems in general.

## INTRODUCTION

The global aerospace community is interested in high altitude, long endurance vehicle technology for missions such as Earth science, remote sensing, communications, and weather and fire monitoring. To date, satellites have provided much of this capability, but new technology has enabled unmanned aerial vehicles (UAVs) to become a viable alternative.

UAVs have several advantages over satellites for these types of missions including lower cost, better maneuverability, and quicker deployability. The lower operational altitude of UAVs helps reduce cost and complexity as well, and also enables larger bandwidth communication connections with ground stations. At the same time, UAVs can fly much longer

duration missions than manned aircraft while carrying no appreciable risk to human life, as well as no mass and volume for life support systems. The advantages of high-altitude flight include a better field of view and lower mean wind speeds at 60,000 - 70,000 feet above sea level. On the other hand, the high altitude carries with it the major challenge of how to power these UAVs, which cannot return to Earth for refueling, during the long duration mission.

The aerospace community has fostered several approaches to meeting the auxiliary power and propulsive power requirements of UAVs for high altitude long endurance missions. For missions of very long duration of 30 days or more, it is not practical to carry on board all of the energy required, assuming that nuclear power is not an option. For these very long missions, the local availability of solar power makes it the most viable option. Of course, solar power is available only in daylight, and must be stored on board for nighttime power usage. One solar-powered vehicle concept that is being explored for the 30+ day mission window is to use solar energy and an energy storage system (involving either rechargeable batteries or regenerative fuel cells) with a flying wing platform (for example, AeroVironment's Helios aircraft, developed in conjunction with NASA [1]). Another concept being explored is to use lighter-than-air vehicles with solar energy and energy storage system (for example, the U.S. Missile Defense Agency's Advanced Concept High Altitude Airship project [2]). The use of solar power/regenerative systems for UAVs means that only enough fuel, used as an energy storage medium (for example, hydrogen), needs to be carried on board to provide power for a single night. However, the drawbacks are the complexity of the combined solar energy conversion and energy storage system, the large size of the energy collector and the variation of incident solar power intensity with latitude and season. For long endurance missions with a mission window of 10 to 20 days, it is possible to use

cryogenic hydrogen and fuel cells on a fixed-wing UAV platform, instead of solar power. Such a system, deriving its power solely from a chemical source all of which is carried on board, does not suffer from the challenges that solar power does. Examples of such UAVs include the cryogenic hydrogen-based PEM fuel cell powered Global Observer UAV of [3], and the 500 W PEM fuel cell powered UAV with metal-hydride hydrogen storage reported in [4].

For UAVs that use solely a chemical energy source to meet their power requirements for a long endurance mission, a large fraction of the take-off mass is the fuel itself, and it is therefore important to use a high specific energy (energy per unit mass) fuel. Hydrogen, with its lower heating value (LHV) of about 120 MJ/kg (compared to that of JP-8, about 43 MJ/kg), is the obvious choice from this perspective. From the perspective of energy density (energy per unit volume), the comparison is different. Compressed gaseous hydrogen, even at very high pressures (700 bar, for example) is much less volumetrically dense when compared to typical room temperature liquid hydrocarbon fuels. Liquid hydrogen is somewhat more compact, but still about four times less dense than JP-8. Liquid hydrogen is chosen for this study; however, further work is needed at the aircraft level of analysis and is discussed further below. The choice of powerplant is another trade-off. Is it better to use a reciprocating internal combustion engine, a gas turbine engine or a fuel cell, to utilize the hydrogen? While a head-to-head comparison of these alternatives is beyond the scope of this paper, we undertook this study to further examine the SOFC approach in particular.

Fuel cells are distinguished from combustion engines by their markedly lesser emission of pollutants and by their potentially high energy conversion efficiency. It seems obvious that a more efficient power system would cut back on the mass of fuel required to produce a prescribed power level for a prescribed duration, and thus allow the aircraft to carry a larger payload. Indeed, most fuel cell systems reported in the literature [cf. 5] to date are developed for land-based power generation, where the power generation systems process enormous quantities of fuel over their operational lifetimes, and where the chief aim is to minimize total cost of electricity. For stationary power generation, the mass and volume of the dry powerplant are not a major consideration, except insofar as they affect construction and housing costs. However, the applicability of fuel cells for aerospace power generation can be quite different. For these applications, the power system must meet strict mass and volume constraints, because it costs fuel to carry fuel and engines into the air and keep them aloft.

First, we briefly discuss the volume constraints. The volume constraints, considered independently of the direct dependence of mass on volume, enter the picture mainly through the extra drag force experienced by the UAV. Increased volume requirements can adversely affect the lift-to-drag ratio of the UAV, by increasing the craft surface area and thus the drag coefficient of even a streamlined UAV. This in turn leads to greater power requirements and greater mass. The volume effects are hard to estimate, depending as they do on

the spatial packaging of the power system components, and on the details of the integration of the power system with the airframe. The design of the airframe and the aerodynamic design of the fuel tank lie outside the purview of this paper. However, we remark that, generally speaking, minimizing the mass of the fueled power system also approximately minimizes its volume (it would exactly minimize the volume if the powerplant and fuel were all of a single uniform density). There is a tradeoff between a design based on minimum power system mass reached without considering volume effects and one based on minimum power system volume, but the two minima will be close to each other in the design space. For example, relative to a minimum mass design that ignores volume effects, trading some low-density fuel mass for a comparable mass of high-density powerplant mass may buy an overall volume decrease which in turn would decrease the drag and the power and thus the total system mass. However, such a trade should produce a minor shift in the design point, and should not affect the conclusions of this study. Based upon these considerations, we do not attempt to analyze the overall volume of the power system, or its effect on system mass, in the current work.

The system mass depends on the system components much more simply than does the system volume: it is simply the sum of the component masses. There are two primary figures of merit related to the power system mass. They are the system specific power and the system specific energy. The system specific power (in units of kW/kg) is the ratio of the net power generated,  $P$ , to the fueled mass of the power system  $M_{fps}$ , i.e., the sum of masses of the dry power system, the total fuel required for the mission, and the fuel tank to contain it. The system specific energy (in units of kJ/kg) is the ratio of the total energy generated,  $E$ , by the power system (during the mission) to the fueled mass of the power system. For any given UAV, with given lift and drag coefficients and planform area of the wing, the propulsive power must be large enough to overcome the drag and propel the vehicle fast enough to provide sufficient lift to support at least the mass  $M_{fps}$  in a gravitational field. If not, the vehicle would fail to stay airborne even if the rest of the vehicle and the payload were massless. An analysis (included as an Appendix) would indicate that this minimum required power varies as  $M_{fps}$  to the exponent 3/2. This carries the implication that if increasingly longer mission durations are considered, requiring increasing fuel mass and correspondingly increasing  $M_{fps}$ , then not only will the minimum required power increase but the minimum required system specific power will also increase. The actual system specific power decreases, however, if we hold the power generation level fixed in an attempt to increase mission duration by increasing only the mass of fuel and fuel tank. Therefore, for missions of long enough duration, the system specific power will fall below its required minimum, and the vehicle will be too heavy with fuel to fly. For such mission durations, we must use solar power with energy storage subsystems. In the current study, we do not perform the overall UAV design that would allow us to estimate the total aircraft mass to be supported by lift, but

instead we focus only on the power generation system. Therefore, we assume that for all the cases we consider, the system specific power constraint is met. In any case, minimizing  $M_{fps}$ , as we aim to do in a future paper, has a beneficial effect on the system specific power, too. When a full-vehicle UAV design is being carried out, of course, the designer must check that the system specific power is high enough to generate sufficient lift for climb. In our study, we prescribe power generation levels which are held constant for the entire duration of the mission, so that our study could apply either to power for onboard instrumentation or to power for propulsion. When the power system is intended to provide power for propulsion, a more accurate estimate of energy requirements (not performed here) would take into account the mission power profile and the decrease in aircraft mass over the mission due to fuel consumption.

Of the two mass-related figures of merit, we focus on the system specific energy. For a prescribed net power level  $P$ , held steady for a prescribed mission duration  $t$ , maximizing the system specific energy is equivalent to minimizing  $M_{fps}$ . Doing this would allow a larger payload to be carried, or make faster forward flight and climb possible. A previous study [6] developed a hybrid SOFC/GT cycle design geared towards aerospace applications. A further study [7] used system component mass models developed in [8] to study the system specific energy of the SOFC/GT system applied to an aircraft auxiliary power unit (APU) delivering 440 kW of power in a Boeing 777 aircraft. In ref. [7], the system specific energy was compared with that of the existing Honeywell APU for that aircraft, which uses a conventional gas turbine (GT). It was found in [7] that despite the considerably higher efficiency of the SOFC/GT as compared with the conventional GT APU, its specific energy was lower than that of the GT. This was true in spite of the aggressive and forward-looking technology assumptions made for the SOFC. This result for the SOFC/GT system was traced to two causes: (a) for the mission durations of 3 and 10 hours considered, the dry mass of the power system formed a large part of the fueled power system mass; consequently the large specific power of the GT system worked in its favor; and (b) the SOFC/GT system used Jet-A as the fuel; consequently a large water mass had to be carried along to prevent coking in the onboard fuel reformer used to convert Jet-A to hydrogen-rich reformat.

In the present study, we avoid the need to carry water for fuel reformation, by using hydrogen directly as fuel. Further, we target long duration UAV missions for the following reason. For long duration missions, with prescribed power generation level, the fueled system mass  $M_{fps}$  will be dominated by the masses of the fuel and fuel tank. Note that the mass of the fuel tank is assumed to scale linearly with the fuel mass, which is a reasonable approximation for exploring this scenario. Let us assume that the system specific power constraint is not violated, and imagine a limiting case of very long duration for which the dry power system mass is practically negligible as compared with the fuel and tank masses. In this limiting case, the system specific energy will be the product of three factors:

the specific energy (LHV) of the fuel, the ratio of fuel mass to the sum of fuel and tank masses, and the energy conversion efficiency of the power system. This limiting system specific energy will be larger than for shorter duration missions in which the power system dry mass also appears in the denominator of the second factor. Clearly, this limiting specific energy can be made higher by picking an energy conversion system of the highest efficiency possible, provided that the dry mass needed to achieve this high efficiency does not have a noticeable impact on  $M_{fps}$ . Note that in the ideal (and impossible) case of negligible tank mass and perfect energy conversion efficiency, the limiting system specific energy is simply the specific energy (LHV) of the fuel. This train of thought led us to explore, in this paper, the possibility that long duration missions may favor more efficient fuel cells in spite of their greater mass.

For the same reason of higher efficiency as mentioned in the previous paragraph, we chose to study an SOFC/GT hybrid system rather than a Proton Exchange Membrane (PEM) fuel cell. The PEM fuel cell operates at a lower temperature, and its waste heat is therefore of lower quality and harder to recover. It is typically liquid cooled using a radiator, which adds mass and causes drag. The SOFC, on the other hand, is cooled by the air flow through the cathode, and thus requires no external radiator. The SOFC also operates at a higher temperature than the PEMFC, and therefore its generated heat and energy of unutilized fuel fraction can be recovered by using a combustor and gas turbine as a bottoming cycle. Such a hybrid thermodynamic cycle can reach very high efficiencies. Indeed some of the highest power system efficiencies reported in the literature [5] have been associated with this type of hybrid power system. Siemens-Westinghouse have reported a 53% overall system efficiency in the first-ever SOFC/GT hybrid system demonstration on a 200 kW system [9].

We employ zero-dimensional steady-state thermodynamic models for the system components, which include the SOFC, the gas turbine, a combustor, an air compressor, a liquid hydrogen tank, a hydrogen vaporizer, and air and fuel preheaters. The thermodynamic system design is followed by component mass and volume sizing, using the previously developed capability, together with some additional newly developed component mass models. We recognize that controls and dynamics of the system may have important effects on the overall design, but here we limit ourselves to steady-state models. The analysis is design-point only, and is performed for operation at the cruise altitude where more than 90% of the UAV flight time is spent. The study [10] showed that off-design system performance analysis is important to the evaluation of sea-level take-off and climb behavior of a system of which the design point is for operation at high altitude. However, we defer such off-design analysis to a future study.

It is our objective in this paper to explore the design trade space for a baseline SOFC/GT system in the 50 kW power class, operating at a cruise altitude of 21 km. We select the fueled power system mass  $M_{fps}$  as the figure of merit that we would like to minimize. To understand the dependence of  $M_{fps}$

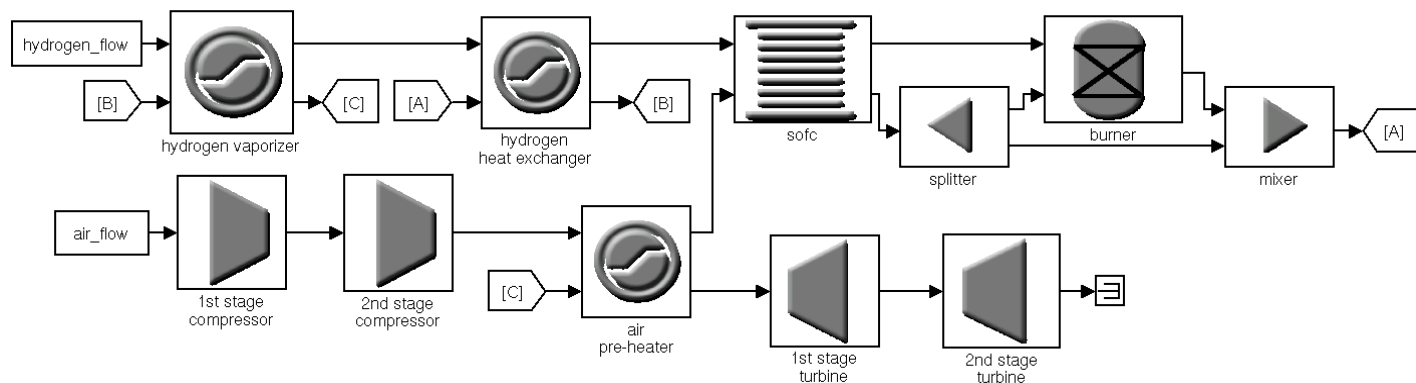


**Figure 1. Schematic diagram of the SOFC/GT hybrid system. The single letter blocks (A, B, C) are used for clarity and show a connection between each other. For example, the ‘A’ blocks indicate a stream from the mixer to the hydrogen heat exchanger.**

on system design and mission, and to provide guidance in future efforts to optimize the system design, we study the variation of  $M_{fps}$  with respect to selected design point and mission parameters. These parameters are the SOFC operating point, the mission duration, the operational altitude and the net developed power. We also study the sensitivities of  $M_{fps}$  to important component parameters such as compressor and turbine efficiency, SOFC area-specific-resistance and SOFC cell support technology.

## NOMENCLATURE

SOFC	solid oxide fuel cell
GT	gas turbine
UAV	unmanned aerial vehicle
LHV	lower heating value
HHV	higher heating value
APU	auxiliary power unit
PEMFC	polymer electrolyte membrane fuel cell
$P$	net system power, kW
$M_{fps}$	mass of the fuel, fuel tank, and power system, kg
$E$	energy generated by the power system, kJ
$t$	mission duration, days
$\eta_{ad}$	Adiabatic efficiency
$\eta$	SOFC LHV efficiency
$\mu_F$	SOFC anode fuel utilization fraction
$V_C$	SOFC cell voltage, V

## SYSTEM DESIGN AND MODELING

### System Configuration

A schematic diagram of the SOFC/GT hybrid system is shown in Figure 1. Liquid hydrogen from a pressurized fuel tank is vaporized and then heated in a heat exchanger to the SOFC operating temperature, and fed to the SOFC anode. Atmospheric ambient air in which the UAV is flying is compressed to the SOFC operating pressure using a two-stage

compressor (each stage is shown as a separate block), heated in a heat exchanger to the SOFC operating temperature, and fed to the SOFC cathode. The anode and cathode outflows are fed to a combustor so that the fuel remaining in the anode stream is combusted to convert its chemical energy into internal energy of the fluid stream. A flow splitter and a flow mixer are used to divert some of the cathode outlet air around the combustor, so that the combustor can operate at unity stoichiometric equivalence ratio. The large enthalpy of the hot gases issuing from the mixer is recovered as much as possible by sequentially using the hot gases to superheat the hydrogen, vaporize the hydrogen, preheat the air flowing from the compressor to the cathode, and finally perform work in a two-stage gas turbine (each stage is shown as a separate block) before exhausting to the ambient atmosphere. The turbine drives both the compressor and an electric generator. In this way, the net power output of the system is all in the form of electric power, which is convenient for routing power to a motor driving a propeller or to electronic instrumentation or communication equipment. An insulated hotbox encloses the SOFC and the combustor to minimize thermal waste. Not all of these system components are represented in the schematic diagram.

### Thermodynamic and Transport System Design

Engineering science has evolved accurate continuum physics models of most macroscopic systems of engineering interest. In the continuum physics description, the changes in the material streams and the interactions of the streams with the components they flow through are governed by balance laws of mass, momentum and energy, and by constitutive equations of the materials involved. The balance laws and constitutive equations incorporate known thermodynamic and transport properties of the solid and fluid materials. The irreversibilities that occur during finite-rate transport of mass, momentum and energy cause the state changes in the material streams to deviate from reversible changes associated with (ideal) quasistatic reversible processes. The irreversibilities are



closely related to spatial and temporal property gradients and boundary conditions imposed by the component passages. Furthermore, the irreversibilities result in entropy generation, which reduces the energy conversion efficiency.

For each system component together with the matter and energy streams that it processes, depending on which quantities are to be solved for from the model, the engineer is usually faced with one of three problems: the rating problem, the inverse rating problem, and the sizing problem.

If the component geometries and materials, the component shaft work and external heat transfer, and the fluid stream inflow conditions are all prescribed, then we would be faced with the forward or rating or off-design performance problem. This involves computation of the changes in fluid composition and properties as the fluid stream passes through the components, based on mass, momentum and energy balances (with or without irreversibility-causing terms) or approximations thereof. At the end of the computation, we would know the fluid properties at outflow from the system, as well as other dependent quantities such as energy efficiencies or losses.

If we prescribed the same quantities as above with the difference that we prescribed, say, fluid outflow conditions instead of fluid inflow conditions, we would be faced with the backward or inverse problem. This can be solved by applying a rootfinding algorithm to the same coupled nonlinear balance laws as in the forward problem. With properly prescribed conditions, both forward and backward problems have unique answers.

In the present study, however, we are faced with the design or sizing problem. Here, we prescribe fluid properties at both inflow and outflow, and seek the component geometries and materials that will produce the prescribed changes in the fluid streams. We are interested in how the component masses, which can be calculated from the geometries and materials, depend on the changes (across the components) that we prescribe in the fluid properties. The design problem is a difficult one, because in general there is no unique answer. For example, a fuel cell and a gas turbine engine can both transform a fuel to an oxidized state. Furthermore, for a given type of component, there is a close relationship between component size, which determines spatial and temporal property gradients, and component efficiency, which is determined by process irreversibilities and energy losses. There is generally a trade-off between the size and the efficiency of any component. We briefly discuss this with respect to the SOFC component, in the results section of this paper.

In the present situation, we solve the design problem by selecting a type of component and then using traditional approximate engineering design procedures to size the component. For each component, based on engineering experience, we first select an efficiency or a loss coefficient to represent the degree of irreversibility for the regime of interest. Making this choice partially decouples the calculation of the system-level thermodynamic model from the component-level sizing and transport models, enabling us to solve them

sequentially. This efficiency or loss coefficient is treated as a technology parameter for the component. We prescribe the inflow or outflow fluid stream conditions and the change in some fluid properties across the component. Of course, in order for the component to be integrated with the rest of the system, these prescribed values have to be consistent with the continuity of the material and energy streams from one component to another, and are therefore not necessarily freely prescribable parameters for each and every component. From these data, based on mass and energy balances, with the loss coefficient taking the place of irreversibilities arising out of transport balances, the heat and work interactions between the fluid stream and the component can be calculated. Then the loss coefficient and the heat and work duties of the component are used to size the component with the aid of approximate engineering transport theory. In the case of some less important components, only the heat and work duties were used in the sizing, which was done for minimum mass. In these cases, the consistency between the loss coefficient of the sized design and the assumed loss coefficient in the thermodynamic model was not checked.

A systematic degree-of-freedom analysis of the system would normally be performed to determine free parameters in the system. However, we informally identified some important free parameters in the system. These are: (1) mission cruise altitude, (2) mission duration, (3) SOFC area-specific-resistance, (4) compressor stage efficiency, (5) turbine stage efficiency, (6) SOFC operational temperature, (7) SOFC operational pressure, (8) mass fraction of cathode effluent that is fed to the combustor, (9) fuel mass flow rate, (10) air mass flow rate, (11) the fraction of SOFC ohmic heat that is assigned to the anode stream, and (12) SOFC active area. However, using a multivariate rootfinding algorithm, the free parameters numbered 8 through 12 are varied so as to meet the following five constraints: (a) combustor runs at stoichiometric equivalence ratio of unity, (b) net electrical power generated by the system is prescribed, (c) the temperature rise across the SOFC stack is limited to 100 K to avoid excessive thermal stresses, (d) the anode and cathode streams leave the SOFC at equal temperatures, and (e) the SOFC cell voltage is prescribed. Effectively, this rootfinding procedure removes the variables numbered 8 through 12 from their roles as free parameters, and creates two new free parameters instead, namely the net system power and the SOFC cell voltage.

### **Thermodynamic Component Models**

The component models all assume uniform material stream conditions at the entry or exit. Energy losses in piping between components are not accounted for. All components are assumed to operate adiabatically, except for the hydrogen tank. The insulated hotbox makes the adiabatic condition realistic for the SOFC and the combustor. The thermodynamic models for most of the components are similar, consisting of mass and energy balances taking into account any assumed loss coefficient. In the case of the combustor and the SOFC, the energy balances include chemical equilibration, i.e., chemical

reactions that proceed to equilibrium. The thermodynamic model used here for the SOFC was developed in [7] by modification of the one developed in [11]. The thermodynamic properties of atmospheric air as a function of altitude above sea level are based on the International Standard Atmosphere.

### Transport and Mass Models

The transport/mass models used here for the SOFC, the combustor, the turbomachinery, and the gas-gas heat exchangers were developed in [8], based partially on standard engineering industrial practice [12-16]. Two-stage turbomachinery was required to accommodate pressure ratios larger than about six. The mass model for the hydrogen vaporizer was adapted from the one for a steam generator, reported in [8]. The metal layer of the fuel tank is sized for strength using hoop stress calculations. The insulation layer of the tank is sized using a one-dimensional conduction approach that restricts the hydrogen boil-off to a prescribed low level. The mass model for the electric generator was approximated based on a couple of commercially installed generators as being about one kg per kW. This level of approximation is sufficient for the generator, which has a fairly small mass.

### Numerical Implementation

The systems analysis has been conducted in the Matlab™ programming environment [17], which is a commercially marketed Rapid Application Development environment. The component thermodynamic and transport/mass models were programmed as Matlab™ functions. In the component models, the evaluation of thermodynamic and transport properties, as well as chemical equilibration, of the fluid mixture streams was accomplished by function calls to Cantera functions written in Matlab™. Cantera [18] is an open-source library of thermodynamic and transport property functions, and includes property databases for a number of important chemicals. Simulink™, a Matlab™ system simulation tool, was used to formulate a block-diagram representation of the interconnected system, which representation is schematically depicted in Figure 1. The Simulink™ representation (termed a Simulink™ model) makes function calls to the component thermodynamic model functions. A Matlab™ script file was written which implements the rootfinding discussed above using a built-in Matlab™ rootfinding function. The script makes batch mode function calls to the Simulink™ model in order to balance the thermodynamic system during the rootfinding. After the thermodynamic system satisfies the constraints, the script makes function calls to the component mass models. The script does all of this for each design space point in a parametric study. Future work will involve automated system parameter optimization for minimum system mass, using gradient-based or evolutionary optimization algorithms available in Matlab™ toolboxes. Figure 1 was output from the Simulink™ representation, and the plots in Figures 2-12 were created in the Matlab™ environment.

## RESULTS AND DISCUSSION

### SOFC Operating Point and Mission Duration

The baseline system design point and mission parameters are shown in Table 1.

SOFC stack-averaged ASR	0.4 Ω-cm <sup>2</sup>
SOFC cell design	anode-supported cell
SOFC anode fuel utilization	0.85
SOFC inlet temperature	973 K
SOFC inlet pressure	101325 Pa
Compressor stage $\eta_{ad}$	0.80
Turbine stage $\eta_{ad}$	0.85
Net system electrical power, $P$	50 kW
Cruise altitude	21 km

**Table 1. Baseline system parameters used in the following parametric studies.**

As seen above, the SOFC anode fuel utilization was fixed at a relatively high value so that most of the energy conversion takes place in the SOFC, although the GT scavenges the heat generated in the SOFC as well as utilizes the remaining fuel fraction. As previously mentioned, the fueled power system mass  $M_{fps}$  was selected as the figure of merit. In all the trade studies that follow, we examine the dependence of  $M_{fps}$  on SOFC operating point and mission duration, in most cases examining how this dependence on these two parameters changes with respect to a third parameter.

The cell voltage  $V_C$  was selected to represent the SOFC operating point. Adapting eqn. 2.5 of [19] to reflect the LHV of hydrogen rather than the HHV,  $\eta = \mu_F V_C / 1.25$ , where  $\eta$  is the SOFC efficiency,  $\mu_F$  is the fuel utilization fraction, and  $V_C$  is the cell voltage. In effect,  $V_C$  represents the efficiency. When  $V_C$  (and thus the efficiency) is low, the SOFC operates with a relatively large current density, accompanied by substantial entropy generation (reflected in the increased ohmic heating and other losses). In this case, the required power level is achieved with a relatively small active area of the SOFC. The mass of the SOFC is very nearly a linear function of the active area. When, on the other hand,  $V_C$  (and thus the efficiency) is high, the SOFC operates with a relatively small current density, with less entropy generation in the form of decreased ohmic heating and other irreversibilities. In this case, the prescribed power level requires a relatively large active area (and thus mass) of the SOFC. As seen from the middle curve in Figure 2, the active area (which is represented by the SOFC mass) is a nonlinear increasing function of the efficiency (which is represented by the cell voltage). In fact, at high efficiency, the function is growing increasingly rapidly, which is due to the fact that it would take an infinite active area and zero current density to achieve reversible lossless operation of the SOFC.

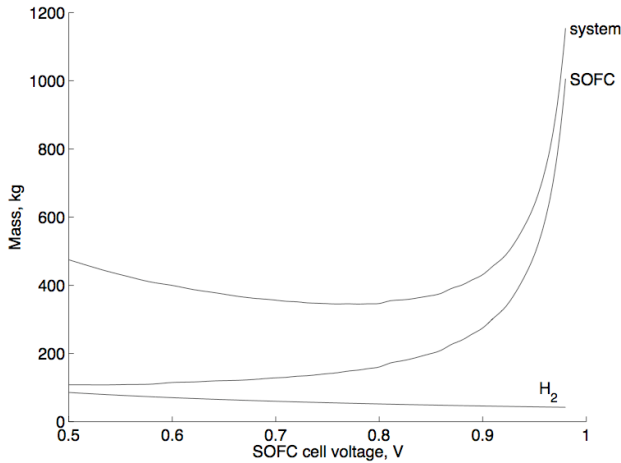


**Figure 2. System, SOFC, and hydrogen mass as a function of SOFC cell voltage for the 1 day mission duration. For this duration, the SOFC is the dominant component mass throughout the range of SOFC cell voltages (and corresponding total SOFC active area). The discrete changes in the SOFC curve are due to the SOFC mass algorithm, where a single stack is limited to 100 cells.**

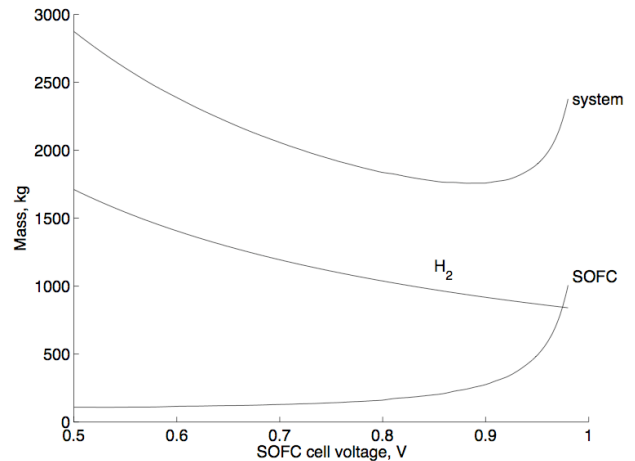


**Figure 3. System, SOFC, and hydrogen mass as a function of SOFC cell voltage for the 20 day mission duration. For this duration, the hydrogen (and its tank, not shown) are the dominant components throughout most of the SOFC cell voltages (and corresponding total SOFC active area).**

Figures 2 and 3 show system, SOFC and hydrogen mass as a function of SOFC cell voltage for the 1 and 20 day mission durations, respectively. It should be noted that the SOFC and hydrogen masses do not add up to the system mass, for there are other component masses that are not shown. For the 1 day duration shown in Figure 2, the SOFC is the dominant component mass throughout the range of the SOFC cell voltage. Yet the fuel and tank masses contribute sufficiently that there is a small advantage to operating the SOFC at a fairly high efficiency, as shown by the shallow minimum of system mass in the vicinity of 0.8 volts. This is already different from the situation encountered with the short duration missions in [7], where it paid to operate the low efficiency, low mass gas turbine rather than the high efficiency, high mass SOFC. The discrete changes at some locations in the SOFC curve are due to the SOFC mass algorithm, where a single stack is limited to 100 cells. The hydrogen mass would be exactly inversely proportional to the cell voltage if the fuel utilization fraction were unity, and is nearly so for the present case, where the utilization is 0.85. The hydrogen curve in Figure 2 looks almost linear over the cell voltage range shown, but its inverse proportionality is seen more clearly in Figure 3. For the 20 day mission duration shown in Figure 3, the hydrogen (and its tank) are the dominant components throughout the SOFC cell voltage range, except at the extremely high voltages at which the very rapid nonlinear growth in SOFC mass overtakes the dropping hydrogen and tank masses. There is thus a sharply defined minimum of system mass occurring at a very high efficiency, which is somewhat higher than the optimum efficiency in the 1

day duration case. For this long duration mission, it pays handsome dividends to operate the SOFC at quite high efficiency and correspondingly high SOFC mass, quite in line with our train of thought in the introduction to this paper. The dependence of fueled power system mass on mission duration can be seen more continuously in the carpet plot to be shown in Figure 6. From that figure, it can be seen that for any prescribed mission duration, the optimum cell voltage is fairly high, and that it increases somewhat with increasing duration. Also, the minimum mass with respect to voltage is much more pronounced at longer durations than at shorter durations. From this, we can draw the conclusion that we can pick the design operating point of the SOFC based on the longest duration mission, and not pay much of a penalty in system mass for the short durations.

The pie chart in Figure 4 shows the breakdown of component masses for the baseline system and a 1 day mission duration. It is seen that the SOFC mass dominates the others, although the hydrogen and tank masses add up to a substantial fraction too.

The pie chart in Figure 5 shows the component masses for the baseline system and a 20 day mission duration. This is a dramatically different plot from the previous one, with the hydrogen and tank masses adding up to what is far and away the largest fraction of the system mass, with the SOFC coming in a distant third. It is immediately apparent from this plot why an increase in SOFC efficiency and mass will yield a large decrease in total mass.

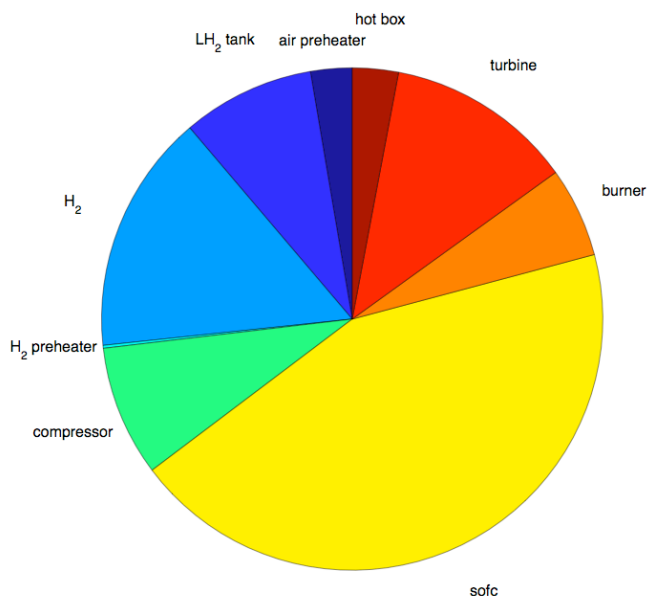


**Figure 4. Pie chart showing relative component masses for the baseline system and a 1 day mission duration.**

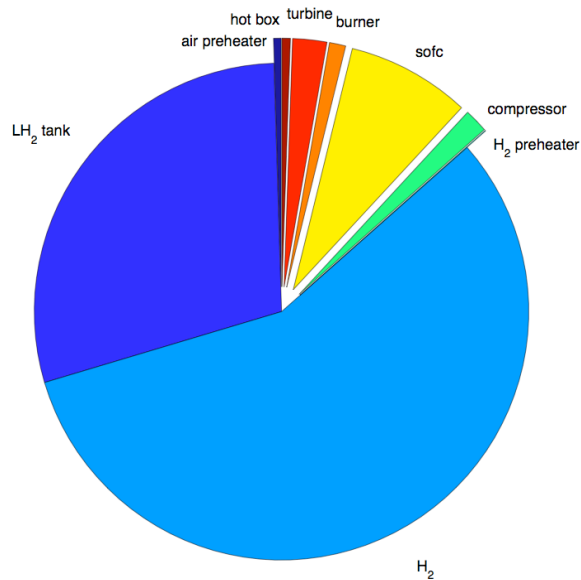


**Figure 5. Pie chart showing relative component masses for the baseline system and a 20 day mission duration.**

The major conclusion from the calculated behavior of the system mass is that a typical long duration mission favors high efficiency and therefore high cell voltage rather than high power density of the dry powerplant. This is the complement to the finding in the earlier commercial aircraft APU study [7], where maximizing power density was the goal due to the shorter mission of 3 to 10 hours. A lower power density is better for SOFC life and reliability, and will enable an earlier introduction of SOFC technology into UAVs, since lower power density SOFCs are already technologically feasible, while higher power densities are still under development.

### Power and Altitude

The carpet plot in Figure 6 shows the variation of system mass with SOFC cell voltage and mission duration, at the baseline power level of 50 kW, and at an altitude of 21 km.

Figure 7 shows system mass as a function of SOFC cell voltage and mission duration, at a power level of 50 kW and an altitude of 16 km. Comparison of Figures 6 and 7 indicates that at least over this range, altitude is not an important factor.

Figure 8 shows system mass as a function of SOFC cell voltage and mission duration, at a power level of 20 kW and an altitude of 21 km. Comparison of Figures 6 and 8 shows that the system mass scales almost linearly with the net system power level. The shape of the system mass surface as a function of voltage and duration is almost unchanged between the two power levels, which fact would be more obvious if Figure 8 used a smaller mass range along the vertical axis. So the system specific power level too is not an important factor in optimizing the system mass. The total system power

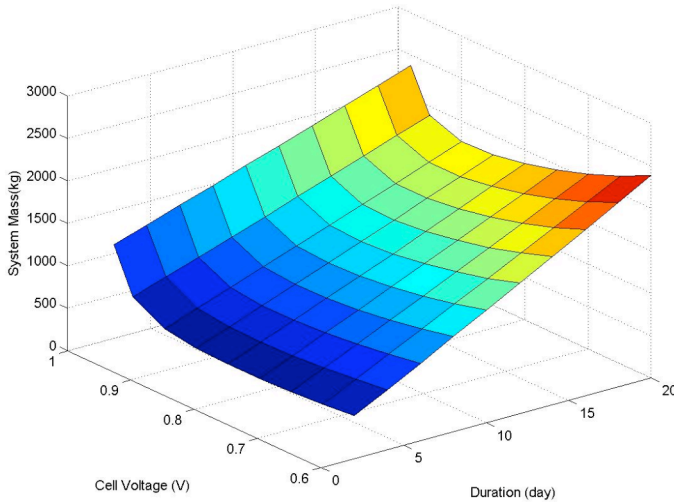
requirement would be based on payload or other extrinsic considerations.

### Sensitivity to Technology Parameters

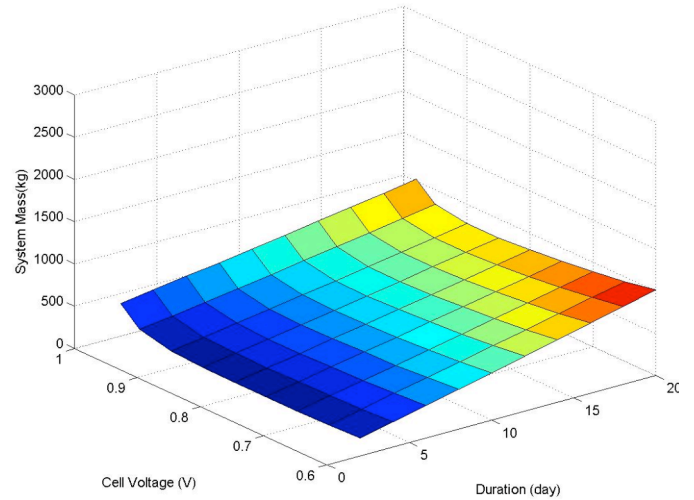
Figure 9 shows the effect of SOFC ASR on overall system mass as a function of SOFC cell voltage and mission duration. As should be expected, an increase in ASR produces an increase in system mass, due to the increase in active area. It also causes the optimum voltage to become somewhat smaller. The change in ASR from the baseline 0.4 to 1.0 has the largest effect at high cell voltages, where the SOFC stack weight is the largest.

Figure 10 shows the effect of the bi-electrode-supported cell (BSC) SOFC design reported in [20], as compared with the baseline anode-supported cell (ASC) design on overall system mass as a function of SOFC cell voltage and mission duration. The BSC design greatly decreases the mass of the interconnect between cells, and thus significantly reduces the SOFC mass.

The turbomachinery efficiency changes, shown in Figures 11 and 12, have the most impact at the low cell voltages, where system efficiency is most important. For low cell voltages, the stack is less efficient and produces more heat and requires more air to cool it, resulting in the need for a larger compressor, which in turn makes the system mass more sensitive to changes in the assumed compressor stage efficiency. For similar reasons, the increase in system mass due to decreased turbine stage efficiency is larger at low cell voltages, because low cell voltages involve a larger turbine to extract power from the larger enthalpy and larger flow rate of the effluent streams from the SOFC. None of the technology parameter perturbations



**Figure 6. Carpet plot showing the system mass as a function of mission duration and SOFC cell voltage (and corresponding total SOFC active area) for a net power level of 50 kW and an altitude of 21km.**



**Figure 8. Carpet plot showing the system mass as a function of mission duration and SOFC cell voltage (and corresponding total SOFC active area) for a net power level of 20 kW and an altitude of 21km.**

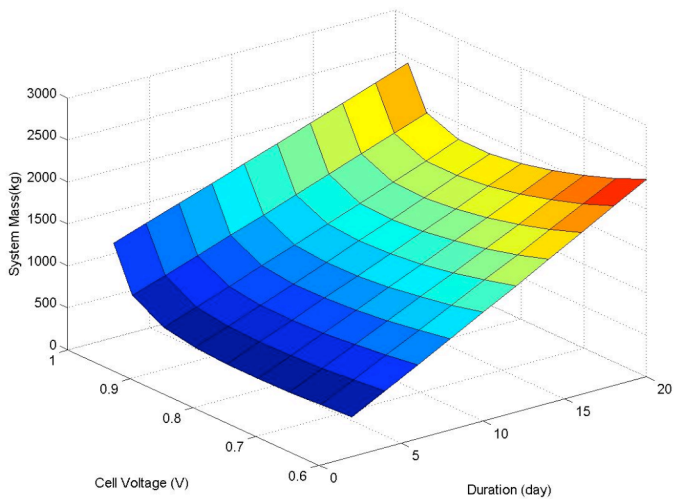


**Figure 7. Carpet plot showing the system mass as a function of mission duration and SOFC cell voltage (and corresponding total SOFC active area) for a net power level of 50 kW and an altitude of 16 km.**

changes the nature of the mass dependency on cell voltage and duration, although they shift the optimum location a little. So the mass dependency behavior is robust with respect to the assumptions on technology parameters.

## CONCLUSIONS

An SOFC/GT hybrid cycle power system was explored for use in high altitude long duration missions of unmanned aerial

vehicles. A system level analysis was performed, which included component mass estimates. The dependence of total fueled power system mass at take-off on the SOFC operating point was examined in the context of varying several system design point and mission parameters. For every mission duration examined in the range of 1 to 20 days, there was a fairly high efficiency optimum SOFC operating voltage that gave the minimum system mass. It was found that long duration missions of the order of 10 to 20 days strongly favored high efficiency, despite the low power density operation of the SOFC. This is in contrast to the situation with missions shorter than half a day, explored in a previous study [7]. Since the minimum is more pronounced for longer durations, the SOFC design point can be set by sizing the active area to produce the optimum cell voltage for the longest duration mission, without paying much of a system mass penalty for shorter durations. The optimality of high efficiency, low power density SOFC/GT operation for long duration UAV missions indicates that SOFC technology could be adopted earlier than expected for UAVs, and that these SOFCs can be expected to have a longer life and higher reliability as a result.

The operating altitude did not have much of an effect on the system mass. The system power level did not affect the type of dependence of system mass on cell voltage and duration, although of course the system mass scales approximately linearly with power level.

The sensitivities of the system mass to technology assumptions such as SOFC ASR and cell interconnect technology, and turbomachinery efficiencies, were evaluated. It was found that the system mass was most sensitive to a change in an SOFC-related parameter at the highest cell voltages, due to the SOFC mass being largest there. The system mass was most sensitive to a change in a

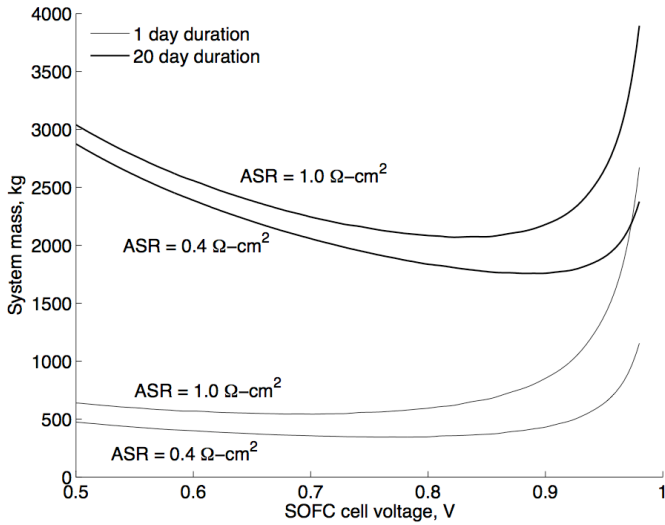


Figure 9. Plot showing the effect of SOFC ASR on overall system mass as a function of SOFC cell voltage (and therefore SOFC total active area) and mission duration.

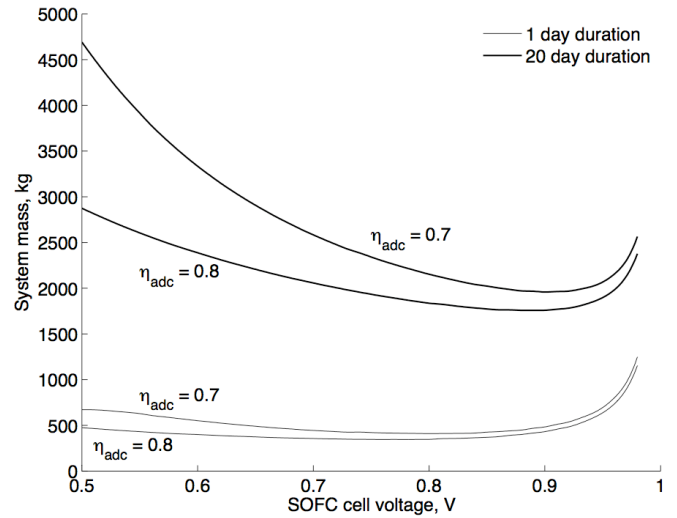


Figure 11. Plot showing the effect of single stage compressor adiabatic efficiency on overall system mass as a function of SOFC cell voltage (and therefore SOFC total active area) and mission duration. Each compressor stage has the specified efficiency.

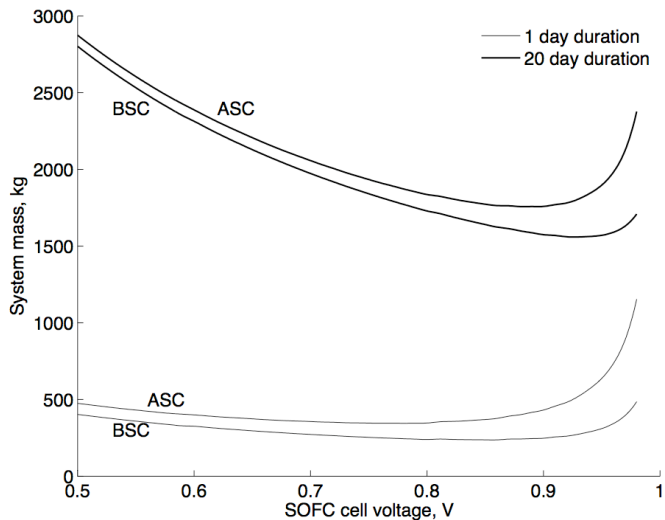


Figure 10. Plot showing the effect of the bi-supported SOFC cell design on overall system mass as a function of SOFC cell voltage (and therefore SOFC total active area) and mission duration.

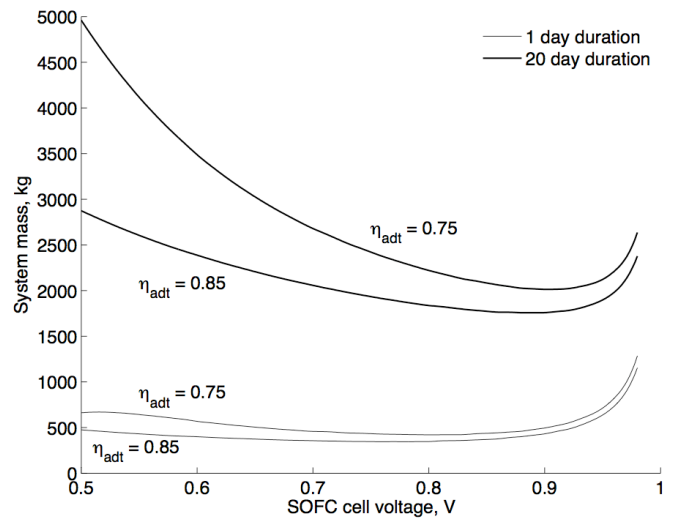


Figure 12. Plot showing the effect of single stage turbine adiabatic efficiency on overall system mass as a function of SOFC cell voltage (and therefore SOFC total active area) and mission duration. Each turbine stage has the specified efficiency.

turbomachinery-related parameter at the lowest cell voltages for the longest duration missions, because operation of the SOFC at low efficiencies caused a lot of heat to be generated in the SOFC, requiring large turbomachinery duties.

In conclusion, the 10 to 20 day UAV mission appears from this system level analysis to be a very promising area for the use of high efficiency, lower power density SOFC/GT hybrid cycle power systems, with the caveat that a complete UAV

design would be needed to verify that these long durations are achievable from a minimum power requirement standpoint.

#### APPENDIX

Consider a UAV in which the only significant mass is that of the fueled propulsive power system,  $M_{fps}$ , at start of mission. Let  $P$  be the power generated by the system at steady horizontal cruise at the start of mission, and  $\eta$  be the efficiency of its

conversion to propulsive power. Let the wing have planform area  $A$ . Let the lift and drag coefficients of the UAV be denoted by  $C_L$  and  $C_D$ , respectively, when the wing is operated at its optimal angle of attack, i.e., to obtain the highest lift-to-drag ratio. Consider steady horizontal cruise of the UAV in a gravitational acceleration  $g$ , at a speed  $U$ , through air of density  $\rho$ . Then, since the lift force serves to support the mass  $M_{fps}$  in the gravitational field,

$$M_{fps}g = \frac{C_L \rho U^2 A}{2}. \quad (1)$$

Since the thrust serves to balance the drag, the propulsive power is the work done against the drag at speed  $U$ . Therefore,

$$\eta P = \frac{C_D \rho U^3 A}{2}. \quad (2)$$

Here,  $P$  is the minimum power required to support  $M_{fps}$  at the start of mission. Eliminating  $U$  between the two equations above,

$$P = \frac{C_D}{\eta} \left[ \frac{2}{\rho A} \right]^{1/2} \left[ \frac{g M_{fps}}{C_L} \right]^{3/2}. \quad (3)$$

## REFERENCES

1. NASA ERAST/Aeroviroment Helios Prototype Aircraft, <http://www.nasa.gov/centers/dryden/history/pastprojects/Erast/helios.html>.
2. U.S. Missile Defense Agency, "High-Altitude Airship", <http://www.mda.mil/mdalink/html/asptaltitude.html>.
3. Dornheim, M.A., (2005), "Fuel Cell Flier", Aviation Week and Space Technology, pp. 52, June 27, 2005, Anthony J. Velocci, Jr., editor, the McGraw-Hill Companies, publisher.
4. Moffitt, B.A., Bradley, T.H., Parekh, D.E., Mavris, D., (2006), "Design and Performance Validation of a Fuel Cell Unmanned Aerial Vehicle", AIAA 2006-823, 44<sup>th</sup> AIAA Aerospace Sciences Meeting and Exhibit, 9-12 January 2006, Reno, Nevada.
5. Fuel Cell Handbook, 7<sup>th</sup> Edition (2004), EG&G Technical Services, Inc., under U.S. Dept. of Energy Contract DE-AM26-99FT40575, National Energy Technology Laboratory, Morgantown, WV, USA.
6. Freeh, J.E., Pratt, J.W., Brouwer, J., (2004), "Development of a Solid-Oxide Fuel Cell/Gas Turbine Hybrid System Model for Aerospace Applications", GT2004-53616, ASME Turbo Expo 2004, Vienna, Austria.
7. Steffen, C.J. Jr., Freeh, J.E., Larosiliere, L.M., (2005), "Solid Oxide Fuel Cell/Gas Turbine Hybrid Cycle Technology for Auxiliary Aerospace Power", GT2005-68619, ASME Turbo Expo 2005, Reno, Nevada.
8. Tornabene, R., Wang, X.-Y., Steffen, C.J. Jr., Freeh, J.E., (2005), "Development of Parametric Mass and Volume Models for an Aerospace SOFC/Gas Turbine Hybrid System", GT2005-68334, ASME Turbo Expo 2005, Reno, Nevada.
9. Veyo, S., Litzinger, K., Vora, S., Lundberg, W., (2002), "Status of Pressurized SOFC/Gas Turbine Power System Development at Siemens Westinghouse", GT2002-30670, ASME Turbo Expo 2002, Amsterdam, the Netherlands.
10. Freeh, J.E., Steffen, C.J. Jr., Larosiliere, L.M., (2005), "Off-Design Performance Analysis of a Solid-Oxide Fuel Cell/Gas Turbine Hybrid for Auxiliary Aerospace Power", FUELCELL2005-74099, Third International Conference on Fuel Cell Science, Engineering and Technology, Ypsilanti, Michigan.
11. Hartvigsen, J., Khandkar, A., Elangovan, S., (1999), "Development of an SOFC Stack Performance Map for Natural Gas Operation", Proceedings of the Electrochemical Society PV 99-19, Honolulu, Hawaii.
12. Wilson, D.G., Korakianitis, T., (1984), The Design of High Efficiency Turbomachinery and Gas Turbines, 2nd Edition, Prentice Hall, Upper Saddle River, New Jersey.
13. Hale, P.L., (1982), "A Method to Estimate Weight and Dimensions of Small Aircraft Propulsion Gas Turbine Engines", prepared for the NASA Lewis Research Center under Contract NASA-23037.
14. Kays, W.M., London, A.L., (1988), Compact Heat Exchangers, 3rd Edition, Krieger, Malabar, Florida.
15. Ganapathy, V., (2003), Industrial Boilers and Heat Recovery Steam Generators: Design, Applications and Calculations, Marcel Dekker, New York.
16. Lefebvre, A.H., (1999), Gas Turbine Combustion, 2nd Edition, Taylor and Francis, Ann Arbor, Michigan.
17. MATLAB Version 7, (2005), The MathWorks, Inc., Natick, Massachusetts.
18. Goodwin, D.G., Cantera, [www.cantera.org](http://www.cantera.org), California Institute of Technology, 2006.
19. Larminie, J., Dicks, A., (2003), Fuel Cell Systems Explained, second edition, John Wiley and Sons, Chichester, England.
20. Farmer, S., Cable, T.L., Sofie, S.W., Steinetz, B., Steffen, C.J. Jr., Kohout, L., Walker, J., (2005), "SOFC for Aerospace Applications at NASA (GRC)", Poster presented at Fuel Cell Seminar, Palm Springs, California, November, 2005.

**REPORT DOCUMENTATION PAGE**Form Approved  
OMB No. 0704-0188

Public reporting burden for this collection of information is estimated to average 1 hour per response, including the time for reviewing instructions, searching existing data sources, gathering and maintaining the data needed, and completing and reviewing the collection of information. Send comments regarding this burden estimate or any other aspect of this collection of information, including suggestions for reducing this burden, to Washington Headquarters Services, Directorate for Information Operations and Reports, 1215 Jefferson Davis Highway, Suite 1204, Arlington, VA 22202-4302, and to the Office of Management and Budget, Paperwork Reduction Project (0704-0188), Washington, DC 20503.

<b>1. AGENCY USE ONLY (Leave blank)</b>		<b>2. REPORT DATE</b> May 2006	<b>3. REPORT TYPE AND DATES COVERED</b> Technical Memorandum	
<b>4. TITLE AND SUBTITLE</b> Hybrid Solid Oxide Fuel Cell/Gas Turbine System Design for High Altitude Long Endurance Aerospace Missions			<b>5. FUNDING NUMBERS</b>  WBS 561581.02.08.03	
<b>6. AUTHOR(S)</b> Ananda Himansu, Joshua E. Freeh, Christopher J. Steffen, Jr., Robert T. Tornabene, and Xiao-Yen J. Wang				
<b>7. PERFORMING ORGANIZATION NAME(S) AND ADDRESS(ES)</b> National Aeronautics and Space Administration John H. Glenn Research Center at Lewis Field Cleveland, Ohio 44135-3191			<b>8. PERFORMING ORGANIZATION REPORT NUMBER</b>  E-15560	
<b>9. SPONSORING/MONITORING AGENCY NAME(S) AND ADDRESS(ES)</b> National Aeronautics and Space Administration Washington, DC 20546-0001			<b>10. SPONSORING/MONITORING AGENCY REPORT NUMBER</b>  NASA TM-2006-214328	
<b>11. SUPPLEMENTARY NOTES</b> Prepared for the Fourth International Conference on Fuel Cell Science, Engineering and Technology sponsored by the American Society of Mechanical Engineers, Irvine, California, June 19-21, 2006. Ananda Himansu, Taitech, Inc., 1430 Oak Court, Suite 301, Beavercreek, Ohio 45430; Joshua E. Freeh, Christopher J. Steffen, Jr., Robert T. Tornabene, and Xiao-Yen J. Wang, NASA Glenn Research Center. Responsible person, Ananda Himansu, organization code RTS, 216-433-5876.				
<b>12a. DISTRIBUTION/AVAILABILITY STATEMENT</b> Unclassified - Unlimited Subject Categories: 07 and 44  Available electronically at <a href="http://gltrs.grc.nasa.gov">http://gltrs.grc.nasa.gov</a> This publication is available from the NASA Center for AeroSpace Information, 301-621-0390.			<b>12b. DISTRIBUTION CODE</b>	
<b>13. ABSTRACT (Maximum 200 words)</b>  A system level analysis, inclusive of mass, is carried out for a cryogenic hydrogen fueled hybrid solid oxide fuel cell and bottoming gas turbine (SOFC/GT) power system. The system is designed to provide primary or secondary electrical power for an unmanned aerial vehicle (UAV) over a high altitude, long endurance mission. The net power level and altitude are parametrically varied to examine their effect on total system mass. Some of the more important technology parameters, including turbomachinery efficiencies and the SOFC area specific resistance, are also studied for their effect on total system mass. Finally, two different solid oxide cell designs are compared to show the importance of the individual solid oxide cell design on the overall system. We show that for long mission durations of 10 days or more, the fuel mass savings resulting from the high efficiency of a SOFC/GT system more than offset the larger powerplant mass resulting from the low specific power of the SOFC/GT system. These missions therefore favor high efficiency, low power density systems, characteristics typical of fuel cell systems in general.				
<b>14. SUBJECT TERMS</b>  Fuel cell; Thermodynamics			<b>15. NUMBER OF PAGES</b> 17	
			<b>16. PRICE CODE</b>	
<b>17. SECURITY CLASSIFICATION OF REPORT</b> Unclassified	<b>18. SECURITY CLASSIFICATION OF THIS PAGE</b> Unclassified	<b>19. SECURITY CLASSIFICATION OF ABSTRACT</b> Unclassified	<b>20. LIMITATION OF ABSTRACT</b>	





